A. Muzhikyan, A. M. Farid, and K. Youcef-Toumi, "Variable Energy Resource Induced Power System Im- balances: A Generalized Assessment Approach," in IEEE Conference on Technologies for Sustainability, (Portland, Oregon), pp. 1–8, 2013.

Variable Energy Resource Induced Power System Imbalances: A Generalized Assessment Approach

Aramazd Muzhikyan
Masdar Institute of
Science and Technology
P.O. Box 54224 Abu Dhabi, UAE
Email: amuzhikyan@masdar.ac.ae

Amro M. Farid
Masdar Institute of
Science and Technology
P.O. Box 54224 Abu Dhabi, UAE
Email: afarid@masdar.ac.ae

Kamal Youcef-Toumi
Massachusetts Institute
of Technology
Cambridge, MA, USA
Email: youcef@mit.edu

***Abstract*—The impact of variable energy resources (VER) on power system operations and planning has been a subject of extensive research in recent years. However, most of the results are based on specific case studies and do not allow generalization. This paper proposes a generalized approach to the assessment of power system imbalances. Penetration level, day-ahead and short-term forecast errors, and variability are identified as four main parameters of VER integration. The dependence of power system imbalances on VER integration parameters is studied, using steady-state simulations. The simulations use a power system enterprise model that consists of three layers: resource scheduling, balancing operations and the physical grid with integrated VER. Resource scheduling is modeled as a security-constrained unit-commitment (SCUC) problem. The balancing layer consists of three components: regulation service, real-time market and operator manual actions. The real-time market is implemented as a security-constrained economic dispatch (SCED) problem. The IEEE RTS96 test system with integrated wind generation is used as the physical grid in the case study.**

***Keywords*—Power system imbalances, wind integration**

I. Introduction

The key findings of recent variable energy resource (VER) integration studies are summarized in [1], [2]. Here, significant wind and solar penetration adds new levels of variability and uncertainty to power systems; thus impeding balanced operations as defined by the North American Electric Reliability Corporation (NERC)'s control performance standards (CPS). The main conclusion of such studies is that renewable energy integration requires provision of additional reserves and regulation. However, most of these results are based on specific case studies that comment on the sufficiency of a power system's flexibility in relation to VER penetration [3], [4], thus limiting their generalizability [5]. Consequently, a recent review has motivated the need for holistic assessment methods [6].

To that effect, this paper seeks to develop a generalized approach to the assessment of power system imbalances. It draws as inspiration the concept of integrated enterprise control in which both physical as well as enterprise processes are modeled to gain an understanding of the holistic system behavior [7]. In such a way, the variability of renewable energy resources can be viewed as an input disturbance which the (enterprise) power system systematically manages to deliver attenuated power system imbalances. Consequently, the power from renewable energy sources is modeled in terms of its key characteristics: penetration level, forecast error, and variability. Furthermore, the enterprise power system modeling includes three layers, namely resource scheduling, balancing actions as well as a physical layer, which represents the buses, transmission lines, loads and generators. While it is not possible within the scope of this paper to model all enterprise power system processes, the ones most relevant to power system imbalances are captured: unit commitment, regulation service, real-time market, and operator manual actions.

This paper studies the impact of VER integration on power system imbalances for varying levels of penetration, forecast error, and variability. This assessment methodology facilitates making case-independent conclusions on how VER impact power system imbalances. The sequel to this paper systematically addresses mitigation strategies. The independent variables in this study are converted to a set of dimensionless numbers to further clarify objective comparison of the results. Finally, imbalances are presented in terms of the corresponding levels of CPS compliance.

II. Background

A. Power System Imbalances

Power generation and consumption balance is one of the main requirements for power system reliable operations. Mismatch between generation and consumption also creates mismatch between mechanical and electrical torques applied on generators. If generation exceeds consumption, generators accelerate, and the system frequency increases. Likewise, if consumption exceeds generation, generators decelerate, and the system frequency decreases. Deviations of the system frequency from the rated value may have damaging effect on power system equipment, that is designed for working at a specific frequency.

The instantaneous power balance in the system with ΔF frequency deviation is given by the following equation [8]:

$$\Delta P_m - \Delta P_D = D_F \Delta F + \frac{dW_k}{dt} \tag{1}$$

where ΔP_m and ΔP_D are changes in mechanical power and electrical power demand correspondingly, D_F is the aggregated damping parameter of generators, and dW_k/dt is the rate of change in kinetic energy.

For a specific control area, power generation and consumption imbalance is called area control error (ACE). ACE is a

crucial parameter of power system imbalance monitoring and performance assessment. For steady-state simulations, dW_k/dt is zero, and Equation (1) takes the following form:

$$ACE = D_F \Delta F \tag{2}$$

Equation (2) is used to measure ACE in real power systems. First, the deviation of the system frequency from rated value is measured, then ACE is calculated from (2).

B. Imbalance Mitigation

Power systems always experience imbalances due to forecasting uncertainties, generator outages, equipment failures and other contingencies. Any imbalance triggers a counter action from the power system to mitigate it. Traditionally, the power system dynamics are classified as a hierarchy of dynamics: primary, secondary and tertiary [9]. Primary dynamics and control address transient stability phenomena in the range of 10-0.1Hz [10]. These represents the inertial response of generators and loads and may be controlled by generator output adjustments implemented by automatic generation control and automatic voltage control [8]. Secondary and tertiary control are managed by independent system operators and balancing authorities and are the main focus of this work. Detailed descriptions of these techniques are presented in the next section.

C. Control Performance Standards

Implementation of all balancing actions, however, does not eliminate imbalances completely. As a matter of fact, ideal generation and consumption balance is not required. The North American Electric Reliability Corporation (NERC) defines the requirements of imbalance mitigation, called control performance standard (CPS) [11]. According to *Standard BAL-001-0.1a*, each balancing authority shall operate such that its average ACE for at least 90% of clock-ten-minute periods (6 non-overlapping periods per hour) during a calendar month is within a specific limit L_{10}. The value of L_{10} is obtained from the system properties. Thus, this standard provides a tool for balancing performance assessment.

III. Methodology and Simulation Setup

The power system enterprise model, used in this study, is comprised of three interconnected layers: the physical grid, resource scheduling and balancing actions. Fig. 1 shows the conceptual diagram of the model.

Resource scheduling occurs prior to the operating day. At this point, the optimal set of generation units for the operating day is defined, along with their schedules. Also, the required reserve amount is scheduled. The scheduled resources are then managed in the real-time to maintain power system balance. Three balancing actions, namely regulation, real-time market and operator manual actions, are implemented. The implementations of balancing actions are described in the following subsections.

A. Resources Scheduling

Reliable operations of the power system start one day prior the operating day with scheduling of necessary resources. As illustrated in Fig. 1, it accomplishes three goals, namely unit commitment, unit scheduling and reserve scheduling.

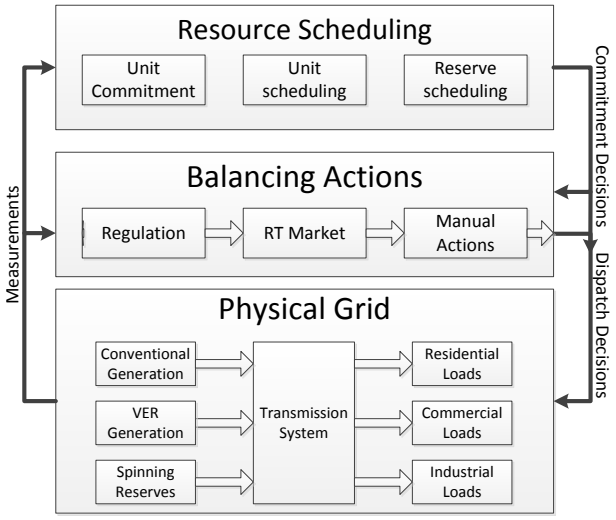

Fig. 1. Conceptual model of a power grid enterprise control simulator

The core component of generation commitment and scheduling is a software-based optimization tool, called Security-Constrained Unit commitment (SCUC), which has a mathematical formulation in the form of linear mixed-integer program [12]:

$$\min \quad \sum_{t=1}^{24}\sum_{i=1}^{N_G}(w_{i,t}C_i^F + C_i^G P_{i,t}^G + w_{i,t}^u C_i^U + w_{i,t}^d C_i^D) \tag{3}$$

$$\text{s.t.} \quad \sum_{i=1}^{N_G} P_{i,t}^G = P_t^D \tag{4}$$

$$-R_i^{G,max}\Delta T \le P_{i,t}^G - P_{i,t-1}^G \le R_i^{G,max}\Delta T \tag{5}$$

$$w_{i,t}P_i^{G,min} \le P_{i,t}^G \le w_{i,t}P_i^{G,max} \tag{6}$$

$$w_{i,t} = w_{i,t-1} + w_{i,t}^u - w_{i,t}^d \tag{7}$$

$$\sum_{i=1}^{N_G} w_{i,t}(P_i^{G,max} - P_{i,t}^G) \ge P^{res} \tag{8}$$

where the following notations are used:

$C_i^F, C_i^G, C_i^U, C_i^D$	fixed, generation (fuel), startup and shutdown costs of generator i
$P_{i,t}^G$	power output of generator i at time t
P_t^D	total demand at time t
$P_i^{G,max}, P_i^{G,min}$	max/min power limits of generator i
$R_i^{G,max}$	maximum ramping rate of generator i
ΔT	scheduling time step, normally, 1 hour
N_G	number of generators
$w_{i,t}$	ON/OFF state of the generator i
$w_{i,t}^u, w_{i,t}^d$	startup/shutdown indicators of generator i
P^{res}	system reserve requirements

The objective of this model is to find the optimal set of generators and their schedules, that will meet the demand with minimal total operating cost of the system. Constraint (4) is the power balance equation, required to keep the system balanced. The other two constraints, (5) and (6), are the physical limitations on generators' ramping rates and power outputs correspondingly. Constraint (8) guarantees the provision of required amount of reserves, where P_{res} is the reserve requirement. The solution of this problem yields optimal $w_{i,t}$ commitment and $P^G_{i,t}$ generation schedules for each generator as well as provision of reserves.

B. Balancing Actions

Day-ahead resource scheduling defines the set of generators available for the operating day. During the operating day, scheduled resources are managed in real-time to ensure balancing of the system at any moment. Fig. 1 shows that balancing actions consist of three components operating at different timescales: regulation, real-time market and operator manual actions. Each component is described in detail in further subsections.

1) Measurement of the Power System State and Imbalances: Effective balancing of the power system requires up-to-date information about system state. In real power systems, this function is carried by the state estimator, which provides information about bus voltages and angles, generation and consumption levels at every bus and the ACE.

Rather than introducing the complexity and errors associated with state estimation implementation, a simpler model of estimating state of the system is used. The values of bus voltages and angles are obtained at every simulation step by running power flow analysis for the given levels of generation and consumption. This gives the exact values of bus voltages and angles, which is similar to perfect state estimation.

Referring to Equation 2, ACE estimation requires measurement of the system frequency deviation. However, for steady-state simulation the concept of frequency is not applicable. Instead, a designated slack generator consumes the mismatch of generation and consumption to make steady-state power flow equations solvable. Therefore, for steady state simulations the power system imbalances are measured as the output slack generator [8].

2) Regulation Service: Generally, regulation service is represented by a dynamic model [13]. However, for steady state simulations a simplified model is implemented. At a time scale slower than 1 minute the effective transfer function simplifies to a gain with saturation limits. Thus, in the current study the regulation is implemented as follows. At each simulation step the regulation service responds to the imbalances by moving its output to the opposite direction. The regulation output changes until imbalance mitigation or regulation service saturation.

3) Real-Time Market: Real-time market operates in parallel to regulation service to suppress imbalances, but in a slower time-scale. It moves available generator outputs to new setpoints in the most cost-efficient way. In its original formulation, generation re-dispatch is implemented as a non-linear optimization model, called AC optimal power flow (ACOPF) [14]. Due to problems with convergence and computational complexity [12], most of the US independent system operators (ISO) moved from ACOPF to linear optimization models. The most commonly used models is Security-Constrained Economic Dispatch (SCED), formulated as incremental linear optimization program [15]:

$$\min \quad \sum_{i=1}^{N_G}(b_i \Delta P^G_{i,t} + 2c_i P^G_{i,t} \Delta P^G_{i,t}) \tag{9}$$

$$\text{s.t.} \quad \sum_{i=1}^{N_B}(1-\gamma_{i,t})(\Delta P^G_{i,t} - \Delta P^L_{i,t}) = 0 \tag{10}$$

$$\sum_{i=1}^{N_B} a_{l,i,t}(\Delta P^G_{i,t} - \Delta P^L_{i,t}) \le F^{max}_l - F_{l,t} \tag{11}$$

$$-R^G_i \Delta t \le \Delta P^G_{i,t} \le R^G_i \Delta t \tag{12}$$

$$P^G_{i,t} - P^{G,min}_i \le \Delta P^G_{i,t} \le P^{G,max}_i - P^G_{i,t} \tag{13}$$

where the following notations are used:

b_i, c_i	generator i offer curve linear and quadratic coefficients
$\Delta P^G_{i,t}, \Delta P^L_{i,t}$	bus i incremental generation and load
$F_{l,t}, F^{max}_l$	line l power flow level and flow limit
N_B	number of buses
$\gamma_{i,t}$	bus i incremental transmission loss factor
$a_{l,i,t}$	bus i generation shift distribution factor to line l
Δt	real-time market time step, normally, 5 minutes.

Use of incremental values for generation and load allows the incorporation of sensitivity factors and the linearization of the program. Sensitivity factors establish linear connections between changes of power injections on buses and state-related parameters of the system [16].

Two sensitivity factors are used in the current model, namely the incremental transmission loss factor (ITLF) and the generation shift distribution factor (GSDF). ITLF for bus i shows how much the total system losses will change, if the injection on bus i increases by a unit [17]:

$$\gamma_{i,t} = \frac{\partial P^{LOSS}_t}{\partial P_{i,t}} \tag{14}$$

where P^{LOSS}_t is total system loss at moment t, $P_{i,t}$ is bus i power injection, both generation and consumption. Incorporation of ITLF into the model results in a linearized power balance constraint (10).

GSDF shows how much line l power flow will change, if injection on bus i increases by a unit [17], [18]:

$$a_{l,i,t} = \frac{\partial F_{l,t}}{\partial P_{i,t}} \tag{15}$$

Incorporation of GDSF into the model results in linearized line flow limit constraint (11).

The other two constraints (12) and (13) are the physical limits of the generator ramping rates and outputs. The objective function in Equation (9) is the minimization of total generation cost. The values for b_i and c_i are linear and quadratic

coefficients of generator offer curves submitted for day-ahead scheduling.

Observation of the model shows that some input parameters, such as $P^G_{i,t}$, $F_{l,t}$, $\gamma_{i,t}$, $a_{l,i,t}$, depend on the current state of the system. These parameters are calculated before each SCED iteration based on full AC power flow analysis of the system. In the literature, this kind of models are referred to as hot start models [15].

4) Operator Manual Actions: In the normal operations mode of the power system, the regulation service and the real-time market are able to maintain the generation and consumption balance effectively. Available generation reserves and generator ramping rates are enough to follow the slowly changing load. However, in the case of contingencies, the situation changes. Sudden outage of a major generation unit creates big imbalances that cannot be mitigated by real-time markets and regulation services. Online generation units do not have enough reserve capacity and enough ramping rates to fill the gap quickly. These kinds of situations require system operator manual actions, in the form of deployment of contingency reserves, decisions on the location of activated reserves, etc. Manual actions, unlike other two components of balancing, have no dedicated operations timescale and are used as necessary.

In the absence of operator models in the literature, their actions are implemented in the following way. The system imbalances are monitored during the interval of simulations. The trigger of operator manual intervention into the balancing procedure works, when the actual imbalances exceed 80% of the largest generation unit. The actions of the operators include balancing of the system manually and bringing new generation units online to suppress imbalances.

IV. The Generation Model of Variable Energy Resources

SCUC and SCED optimization programs, presented in previous sections, are traditional scheduling and balancing tools, without a specific accent on VER integration. However, due to its non-dispatchability, variability and uncertainty, it has similar properties with the system load. Therefore, VER generation is usually considered as negative load on a specific bus, and load component in SCUC and SCED models is replaced with net load:

$$P^{net}_{i,t} = P^{L}_{i,t} - P^{VER}_{i,t} \tag{16}$$

Similar to the load, two types of VER data are used for simulations: VER output forecast data, which is used in optimization models, and actual VER output data, which is used to assess actual state of the system. For this study it is assumed that load has no forecast error, so that all imbalances are results of VER generation. The connection between actual and forecasted VER generation can be expressed as follows:

$$P_{VER}(t) = P^F_{VER}(t) + e(t) \tag{17}$$

where $P_{VER}(t)$ and $P^F_{VER}(t)$ are the actual and forecasted VER generation accordingly, and $e(t)$ is the error term.

Four main parameters of VER are indicated, that can potentially affect the imbalances of the system: penetration level, day-ahead forecast error, short-term forecast error and variability. Changes of these parameters create different VER profiles and, as a result, different integration scenarios. In accordance to these four parameters, four integration scenarios are designed. Definitions of these parameters and incorporation into the wind power model are represented in the following subsections.

A. Penetration Level

In the current study, the penetration level is defined as the ratio of total installed VER capacity to the annual peak load, similar to reference [19]:

$$PEN = P^{max}_{VER} / P^{peak}_{L}. \tag{18}$$

Using this definition, VER generation can be expressed in the following way:

$$\begin{aligned} P_{VER}(t) &= \frac{P_{VER}(t)}{P^{max}_{VER}} \cdot \frac{P^{max}_{VER}}{P^{peak}_{L}} \cdot P^{peak}_{L} = \\ &= \overline{P_{VER}}(t) \cdot PEN \cdot P^{peak}_{L} \end{aligned} \tag{19}$$

where $\overline{P_{VER}}(t)$ is VER power, normalized to unit installed capacity. Equation (19) shows, that VER generation profiles for different penetration levels can be obtained from a single normalized profile. This approach is very useful for running simulations with different penetration levels.

B. Forecast Error

Two types of forecasts are used in the power system simulations, day-ahead and short-term. The day-ahead forecast is used in the SCUC model for day-ahead resource scheduling. It normally has a 1 hour resolution and up to 48 hours forecast horizon. The short-term forecast is used in the SCED model for real-time balancing operations. It has a 10 minute time resolution and up to 6 hour time horizon [20].

Forecast error can be defined in different ways, such as mean absolute error (MAE), mean square error (MSE), etc [21]. It is often convenient to use normalized values of forecast error, by dividing it by installed VER capacity. For simplicity of calculations, in this research, the forecast error is defined as the normalized standard deviation of errors (NSDE) (17):

$$ERR = \frac{\sigma\left(e(t)\right)}{P^{max}_{VER}} \tag{20}$$

where $\sigma\left(e(t)\right)$ is the standard deviation of the error term in (17). This definition of forecast error allows representation of error term in the following way:

$$\begin{aligned} e(t) &= \frac{e(t)}{\sigma\left(e(t)\right)} \cdot \frac{\sigma\left(e(t)\right)}{P^{max}_{VER}} \cdot \frac{P^{max}_{VER}}{P^{peak}_{L}} \cdot P^{peak}_{L} = \\ &= \overline{e}(t) \cdot ERR \cdot PEN \cdot P^{peak}_{L} \end{aligned} \tag{21}$$

where $\overline{e}(t)$ is the forecast error term, normalized to unit standard deviation. An interesting fact follows from Equation (21), that the error term increases with both the increase of forecast error and penetration level. This allows generation of different simulation scenarios by independently varying these two parameters.

Equation (21) is used for both day-ahead and short-term forecast errors. However, the normalized error term $\overline{e}(t)$ is different for these two cases. This separation is absolutely necessary, since they may differ by their probability distribution and power spectra. Also, for these two forecasts, forecast error ranges are different. Normally, short-term forecast error has higher accuracy compared to day-ahead forecast.

C. Variability

Variability is the fourth parameter of VER studied in this work. To the knowledge of the authors, there is no mathematical formulation of variability in the existing literature. In this section a mathematical definition of variability is introduced and its impact VER generation model is presented.

Intuitively, variability should describe how quickly VER changes its output. To establish that connection, the derivative of the power output is used:

$$R_{VER}(t) = \frac{dP_{VER}(t)}{dt} \tag{22}$$

Based on its definition, $R_{VER}(t)$ should be zero-mean random process, otherwise VER output would tend to infinity, which is not possible. Thus, the probability density function (PDF) of $R_{VER}(t)$ actually shows how quick the output of VER can change.

Based on the definition in equation (22), the variability of VER is defined as follows:

$$VAR = \frac{\sigma\left(R_{VER}(t)\right)}{P_{VER}^{max}} \tag{23}$$

where $\sigma\left(R_{VER}(t)\right)$ is the standard deviation of $R_{VER}(t)$. The definition includes normalization to installed capacity, since $R_{VER}(t)$ proportionally increases with penetration level. Unlike the two other parameters, variability has a measurement unit, which is the inverse of time. Simple derivations using Parseval's theorem leads to the following representation of variability:

$$VAR = \frac{\sigma\left(R_{VER}(t)\right)}{P_{VER}^{max}} = \frac{\sqrt{\int_{-\infty}^{+\infty} \omega^2 G(\omega)\mathrm{d}\omega}}{P_{VER}^{max}} \tag{24}$$

where $G(\omega)$ is the power spectral density (PSD) of VER output. This definition of variability can be applied to not only VER, such as wind, solar, but also the system of the load.

The numerator of Equation (24) shows, that variability is proportional to the width of the power spectrum: the wider the spectra, the higher variability. Since VER power spectra mostly have fixed shapes [22], [23], the spectra for different variability levels represent stretched or squeezed copies of each other. This transformation corresponds to a change of the time scaling. It applies on both VER output and the error term:

$$P_{VER}(t) = \overline{P_{VER}}(\alpha t) \cdot PEN \cdot P_L^{peak} \tag{25}$$

$$e(t) = \overline{e}(\alpha t) \cdot ERR \cdot PEN \cdot P_L^{peak} \tag{26}$$

where α is the scaling factor. The higher scaling factor, the higher resulting VER variability. The dependence is linear:

$$\alpha = \frac{VAR}{VAR_0} \tag{27}$$

where VAR_0 is the variability of $\overline{P_{VER}}(t)$.

D. The model of Variable Energy Resources

As already stated above, the simulations of VER integration require two sets of data: actual and forecasted VER output. The derivations from the previous subsections can be summarised in the following models for actual and forecasted VER:

$$P_{VER}(t) = \overline{P_{VER}}(\alpha t) \cdot PEN \cdot P_L^{peak} \tag{28}$$

$$P_{VER}^{F}(t) = \left(\overline{P_{VER}}(\alpha t) - ERR \cdot \overline{e}(\alpha t)\right) \cdot PEN \cdot P_L^{peak} \tag{29}$$

$$\alpha = VAR/VAR_0 \tag{30}$$

This set of equations defines the continuous-time VER model used in the current study. As an input, it requires the actual VER profile $\overline{P_{VER}}(t)$ normalized to installed capacity, and the error term profile $\overline{e}(t)$, normalized to unit standard deviation. The model explicitly includes four major parameters of VER identified for this study. For computer simulations, discrete-time version of the model is implemented, which is described in the next subsection.

V. Case Study

The proposed assessment method is tested for different scenarios of wind power integration. Four different integration scenarios are simulated. During each scenario, one of four VER parameters is changed within a reasonable range holding all others constant. This approach allows the study of the impact of a particular parameter on the imbalances of the system. The performance of balancing actions is evaluated by compliance to CPS's.

Prior to assessing these four scenarios, a traditional power grid without wind integration is simulated to determine the amount of reserves and regulation the traditional system needs to maintain system balance. This approach ensures that imbalances are result of wind integration.

The scenarios are implemented as steady-state simulations in the Matlab environment. The simulations run for one week period with a time step of 1 minute that corresponds to the regulation timescale. It is assumed that faster dynamics are mitigated by inertia response of generation and demand resources.

A. Test System

The IEEE RTS-96 reliability test system is used as the physical grid model [24]. It is composed of three nearly identical control areas, with a total of 73 buses and 99 generators. The yearly peak load is 8550MW.

B. Incorporation of Wind and Load Data

Wind and load data from Bonneville Power Administration repositories [25] are used for the current case study. The best available data has a 5-minute resolution which does not satisfy the requirement of simulations with 1-minute time step. This difficulty is overcome by up-sampling the available data to 1-minute resolution. The up-sampling process is performed with use of *sinc* functions to not introduce distortions into the power spectrum and not change the spectral width [26].

Besides the four parameters discussed above, the VER integration into the actual physical system requires an allocation to system buses. This choice defines potential congestion occurrences which may significantly alter the results of imbalances for the same scenario. Since congestions are outside the scope of this research, the VER capacity distribution is implemented in a way that minimizes congestion probabilities: wind generation on each bus is proportional to the system load on that bus. As a first analysis, the temporal power generation profile of each wind turbine across the topology is assumed to be entirely correlated spatially. Future work can generalize this model to investigate systematic approaches to partial geographic correlation to confirm recent empirical evidence in this regard [27]. Because all the VER profiles are temporally correlated, they have the same variability, and forecast error. This facilitates addressing these parameters as single values across the power system.

C. Simulation Scenarios

Four scenarios are simulated to study the impact of wind power integration on the power system imbalances. During each scenario, the impact of changing one parameter on imbalances is studied, holding the others constant. Brief descriptions of each scenario are presented in the following paragraphs.

Scenario 0: Balancing of the traditional power system. The traditional power system is simulated without wind integration. This is the base case and defines reserve and regulation requirements for balancing the traditional system.

Scenario 1: The impact of wind penetration level *ceteris paribus*. The penetration level ranges from 0% to 20% of annual peak load. This scenario shows how much wind power the traditional system can accommodate, while maintaining CPS requirements.

Scenario 2: The impact of wind variability *ceteris paribus*. The wind variability increases from its default value by a factor of two and three. This scenario shows how the wind pattern may impact the integration experience.

Scenario 3: The impact of wind day-ahead forecast error *ceteris paribus*. The day-ahead forecast error ranges from 0% to 10% of installed wind capacity. This scenario shows the actual benefits that improved wind forecast may bring into the system.

Scenario 4: The impact of wind short-time forecast error *ceteris paribus*. The day-ahead forecast error ranges from 0% to 5% of installed wind capacity. The range here is smaller because short-term forecast error typically has better prediction accuracy.

VI. Simulation Results and Discussion

In the base case scenario, the traditional power system is considered. The goal is to find the reserve and regulation amount necessary to keep the system balance at the required level. Thus, the optimizations are carried in two stages.

The first stage tests the system imbalances for incremental values of reserves. The results are presented in Fig. 2, where the horizontal axis is the reserve requirements, normalized to the system peak load. The performance of the system without any reserve and regulation is close to zero. Later, increase of reserve requirements also increases CPS index. However, the improvements go to saturation when amount of reserves reaches 0.027. Since further increase of reserves does not contribute to effective balancing, the amount of reserves is fixed at that level. Interestingly, the 81% saturation level is below the required 90% level. This is explained by the fact that load variability exists on all timescales. Reserve capacity can only mitigate imbalances slower than the real-time market step. Further improvements should be done by the regulation service.

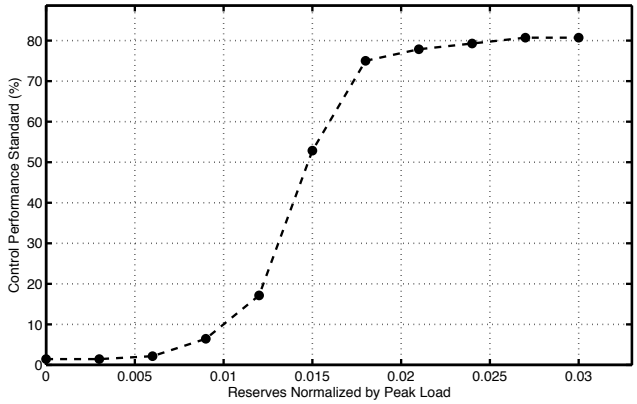

Fig. 2. Traditional power system reserve requirement calculation

The second stage of the bas case scenario adds regulation to the traditional system. Further improvement of balancing performance is recorded as regulation amount increases. The horizontal axis is the regulation amount normalized by the system peak load. Fig. 3 shows that CPS index crosses the required 90% level at regulation value of 0.0008. This value is also fixed for the rest of the scenarios.

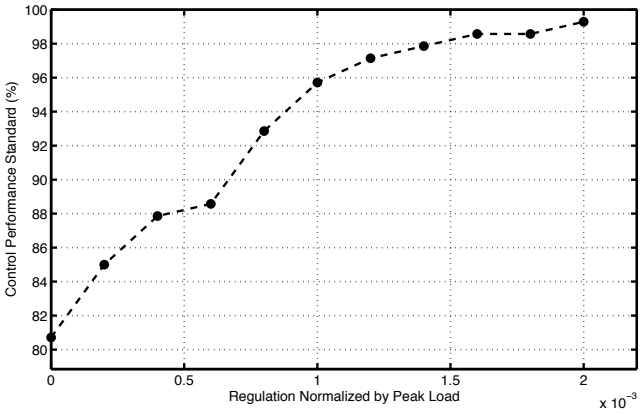

Fig. 3. Traditional power system regulation requirement calculation

The first scenario tests the impact of wind penetration level on the imbalances. For this scenario, the wind is assumed to have a perfect forecast. In this case, only the introduced additional variability may affect the performance of the balancing actions. Fig. 4 shows the decay of the CPS index as wind integration increases. The horizontal axis represents the normalized penetration level as defined in Equation (18). Note

that at the beginning of the simulation the performance of the the system improves a little, which seems to be inconsistent with the rest of the graph. At a low level of penetration, the wind variability may be comparable to the load variability. From that perspective, it is possible that the net load variability actually decreases over the first few points in the simulation.

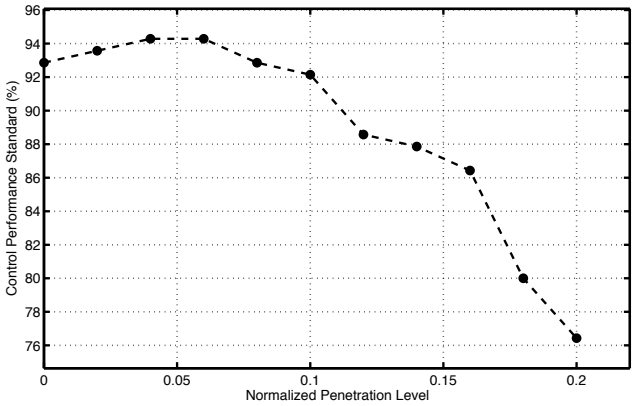

Fig. 4. Power system imbalances for different levels of wind integration

The second scenario further emphasises the impact of wind variability. While keeping the penetration level fixed at 20% level, the variability increases from its default value 2 and 3 times. Unlike other scenarios, the wind variability is only tested for a few values. This is because the discrete domain implementation of Equation 25 only allows for integer scale changes. The results found in Fig. 5 show a doubling of variability drops the CPS value to around 30%. This is an indication that the system experiences severe lack of ramping capabilities. Interestingly, further increases in variability result in limited further degradation of the CPS index. This is because, in both cases, these system is not able to cope with the variability and is constantly out of balance.

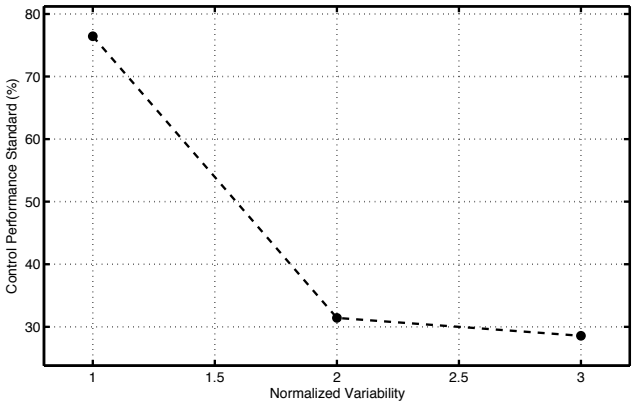

Fig. 5. Power system imbalances for different levels of wind variability

The previous two scenarios demonstrated that even in the case of perfect forecast, the system performance suffers due to wind high variability. In the third scenario, the day-ahead forecast error is added to the wind generation. Building off the 20% wind penetration level, Fig. 6 shows a steep drop of the CPS index as the forecast error approaches 10%. The horizontal axis represents the day-ahead forecast error as defined in (20).

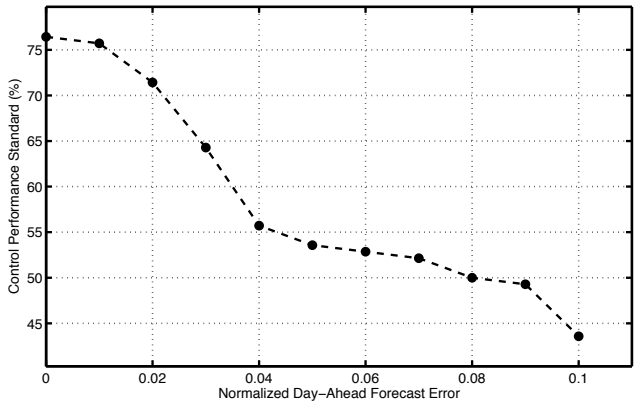

Fig. 6. Power system imbalances for different values of wind day-ahead forecast error

The fourth and final scenario tests the impact of short term forecast error on the imbalances. Building off the 20% wind penetration level and 10% day ahead forecast error, Fig. 7 shows that that after the introduction of the short-term forecast error, the performance of the system balancing drops drastically to a level below 25%.

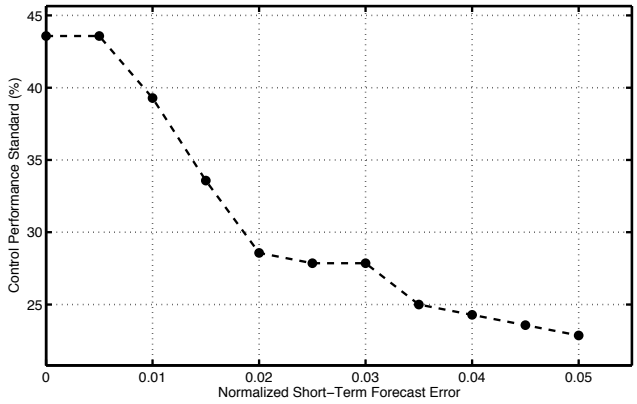

Fig. 7. Power system imbalances for different values of wind short-term forecast error

Thus, wind integrations into the power system brings new levels of variability and uncertainty. As the case study shows, both variability and uncertainty create significant imbalances in the system. This problem occurs because reserves and regulation requirements were calculated based on a traditional power system. To be able to maintain the system balance in the presence of, additional reserves, regulation and system flexibility should be procured. Estimation of these parameters in the case of VER integration is the subject of the sequel paper [28].

VII. Conclusion

This paper has proposed a generalized approach to the power system imbalance assessment. The power system is

modelled as an integrated enterprise consisting of three layers, namely resource scheduling, balancing actions and the physical grid. The balancing layer consists of the real-time market, the regulation service and operator manual actions. These three components work in parallel on different timescales to maintain the balance of the system.

The proposed method is tested on a wind integration case study. Four parameters of wind are identified and their impacts on power system imbalances are tested. The parameters are penetration level, variability, day-ahead and short-term forecast errors. For each of the simulation scenarios, one parameter varies holding the others constant.

The results show that wind integration generally tends to increase the system imbalances. For the first two scenarios, the penetration level and variability impacts are tested. The simulations show that the system experiences a lack of ramping capabilities, which is reflected in the reduction of balancing performance. The other two scenarios test the impacts of day-ahead and short-term forecast errors. These two scenarios indicate a high sensitivity of balancing performance to uncertainties of wind. Thus, the impact of VER on the imbalances may arise from either the variability or uncertainty of the VER.

REFERENCES

[1] E. Ela, B. Kirby, E. Lannoye, M. Milligan, D. Flynn, B. Zavadil, and M. O'Malley, "Evolution of operating reserve determination in wind power integration studies," in *Power and Energy Society General Meeting, 2010 IEEE*, 2010, pp. 1–8.

[2] H. Holttinen, M. Milligan, E. Ela, N. Menemenlis, J. Dobschinski, B. Rawn, R. J. Bessa, D. Flynn, E. Gomez-Lazaro, and N. K. Detlefsen, "Methodologies to Determine Operating Reserves Due to Increased Wind Power," *Sustainable Energy, IEEE Transactions on*, vol. 3, no. 4, pp. 713–723, 2012.

[3] A. Robitaille, I. Kamwa, A. Oussedik, M. de Montigny, N. Menemenlis, M. Huneault, A. Forcione, R. Mailhot, J. Bourret, and L. Bernier, "Preliminary Impacts of Wind Power Integration in the Hydro-Quebec System," *Wind Engineering*, vol. 36, no. 1, pp. 35–52, Feb. 2012. [Online]. Available: http://dx.doi.org/10.1260/0309-524X.36.1.35

[4] T. Aigner, S. Jaehnert, G. L. Doorman, and T. Gjengedal, "The Effect of Large-Scale Wind Power on System Balancing in Northern Europe," *Sustainable Energy, IEEE Transactions on*, vol. 3, no. 4, pp. 751–759, 2012.

[5] M. H. Albadi and E. F. El-Saadany, "Comparative study on impacts of wind profiles on thermal units scheduling costs," pp. 26–35, 2011.

[6] A. M. Farid, "The Need for Holistic Assessment Methods for the Future Electricity Grid," in *GCC CIGRE Power 2013*, Abu Dhabi, UAE, 2013, pp. 1–12.

[7] P. Martin, "The Need for Enterprise Control," *InTech*, vol. Nov/Dec, pp. 1–5, 2012.

[8] A. Gómez-Expósito, A. J. Conejo, and C. Cañizares, *Electric Energy Systems: Analysis and Operation*. Boca Raton, Fla: CRC, 2008.

[9] M. D. Ilic and J. Zaborszky, "Dynamics and control of large electric power systems," pp. xviii, 838 p., 2000. [Online]. Available: http://www.loc.gov/catdir/description/wiley031/99029004.html http://www.loc.gov/catdir/toc/onix01/99029004.html

[10] P. Kundur, N. J. Balu, and M. G. Lauby, *Power system stability and control: The EPRI power system engineering series*. New York: McGraw-Hill, 1994. [Online]. Available: http://www.loc.gov/catdir/toc/mh022/93021456.html http://www.loc.gov/catdir/enhancements/fy1012/93021456-b.html

[11] North American Electric Reliability Corporation, "Reliability Standards for the Bulk Electric Systems of North America," *NERC Reliability Standards Complete Set*, pp. 1–10, 2012. [Online]. Available: http://www.nerc.com/files/Reliability_Standards_Complete_Set_1Dec08.pdf

[12] S. Frank and S. Rebennack, "A Primer on Optimal Power Flow: Theory, Formulation, and Practical Examples," Colorado School of Mines, Tech. Rep. October, 2012.

[13] F. Milano, *Power system modelling and scripting*, 1st ed. New York: Springer, 2010.

[14] J. Carpentier, "Contribution to the economic dispatch problem," *Bull. Soc. Franc. Electr.*, vol. 3, no. 8, pp. 431–447, 1962.

[15] B. Stott, J. Jardim, and O. Alsaç, "DC Power Flow Revisited," *Power Systems, IEEE Transactions on*, vol. 24, no. 3, pp. 1290–1300, 2009.

[16] A. J. Wood and B. F. Wollenberg, *Power generation, operation, and control*, 2nd ed. New York: J. Wiley & Sons, 1996. [Online]. Available: http://www.knovel.com/knovel2/Toc.jsp?BookID=2062

[17] K.-S. Kim, L.-H. Jung, S.-C. Lee, and U.-C. Moon, "Security Constrained Economic Dispatch Using Interior Point Method," in *Power System Technology, 2006. PowerCon 2006. International Conference on*, 2006, pp. 1–6.

[18] L. S. Vargas, V. H. Quintana, and A. Vannelli, "A Tutorial Description of an Interior Point Method and Its Applications to Security-Constrained Economic Dispatch," *Power Systems, IEEE Transactions on*, vol. 8, no. 3, pp. 1315–1324, 1993.

[19] C. Wang, Z. Lu, and Y. Qiao, "A Consideration of the Wind Power Benefits in Day-Ahead Scheduling of Wind-Coal Intensive Power Systems," *Power Systems, IEEE Transactions on*, vol. 28, no. 99, p. 1, 2012.

[20] G. Giebel, R. Brownsword, G. Kariniotakis, M. Denhard, and C. Draxl, "The State-Of-The-Art in Short-Term Prediction of Wind Power: A Literature Overview," ANEMOS.plus, Tech. Rep., 2011.

[21] C. Monteiro, R. Bessa, V. Miranda, A. Botterud, J. Wang, and G. Conzelmann, "Wind Power Forecasting: State-of-the-Art 2009," Argonne National Laboratory, Illinois, Tech. Rep., 2009. [Online]. Available: http://www.osti.gov/energycitations/product.biblio.jsp?osti_id=968212

[22] J. Apt, "The spectrum of power from wind turbines," *Journal of Power Sources*, vol. 169, no. 2, pp. 369–374, Jun. 2007. [Online]. Available: http://www.sciencedirect.com/science/article/pii/S0378775307005381

[23] A. E. Curtright and J. Apt, "The character of power output from utility-scale photovoltaic systems," *Progress in Photovoltaics: Research and Applications*, vol. 16, no. 3, pp. 241–247, May 2008. [Online]. Available: http://doi.wiley.com/10.1002/pip.786

[24] C. Grigg, P. Wong, P. Albrecht, R. Allan, M. Bhavaraju, R. Billinton, Q. Chen, C. Fong, S. Haddad, S. Kuruganty, W. Li, R. Mukerji, D. Patton, N. Rau, D. Reppen, A. Schneider, M. Shahidehpour, and C. Singh, "The IEEE Reliability Test System-1996. A report prepared by the Reliability Test System Task Force of the Application of Probability Methods Subcommittee," *Power Systems, IEEE Transactions on*, vol. 14, no. 3, pp. 1010–1020, 1999.

[25] Bonneville Power Administration, "WIND GENERATION & Total Load in The BPA Balancing Authority." [Online]. Available: http://transmission.bpa.gov/business/operations/wind/

[26] A. V. Oppenheim and R. W. Schafer, *Discrete-Time Signal Processing*, 3rd ed. Prentice Hall, 2010.

[27] M. Milligan, K. Porter, E. DeMeo, P. Denholm, H. Holttinen, B. Kirby, N. Miller, A. Mills, M. O'Malley, M. Schuerger, and L. Soder, "Wind power myths debunked," *Power and Energy Magazine, IEEE*, vol. 7, no. 6, pp. 89–99, 2009. [Online]. Available: http://dx.doi.org/10.1109/MPE.2009.934268

[28] A. Muzhikyan, A. M. Farid, and K. Youcef-Toumi, "Variable Energy Resource Induced Power System Imbalances : Mitigation by Increased System Flexibility , Spinning Reserves and Regulation," in *IEEE Conference on Technologies for Sustainability*, no. 1, Portland, Oregon, 2013, pp. 9–16.